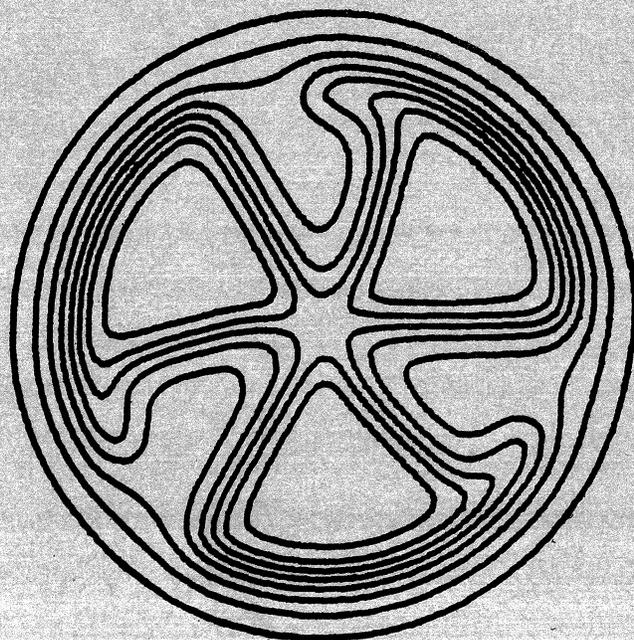


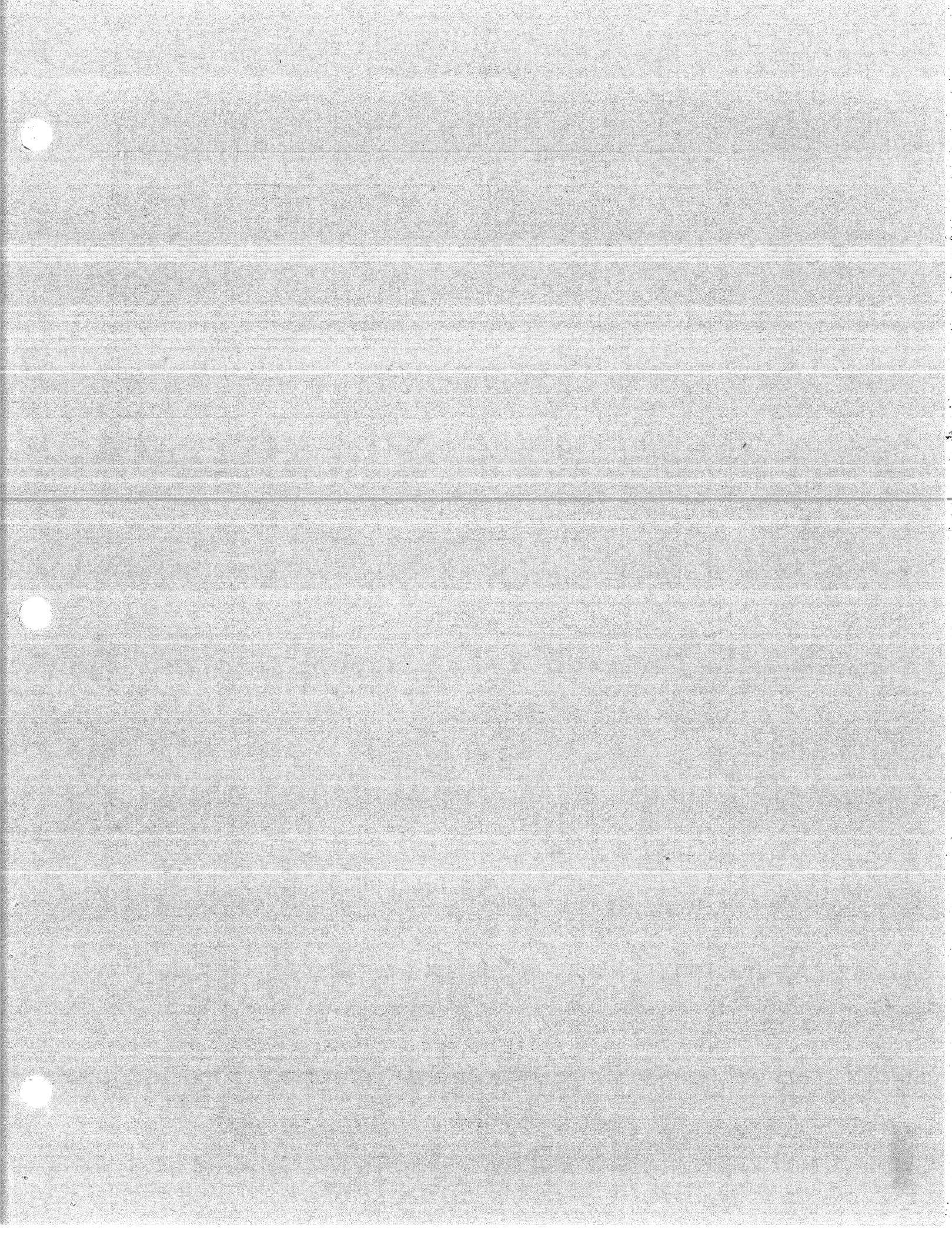
MICHIGAN STATE UNIVERSITY

CYCLOTRON LABORATORY

STUDY OF THE $^{64}\text{Ni}(p,t)^{62}\text{Ni}$ REACTION

D.H. KONG-A-SIOU and H. NANN





Study of the ${}^{64}\text{Ni}(p,t){}^{62}\text{Ni}$ Reaction[†]

D. H. Kong-A-Siou* and H. Nann
Cyclotron Laboratory, Michigan State University
East Lansing, Michigan 48824

ABSTRACT

Energy levels in ${}^{62}\text{Ni}$ up to an excitation energy of 6.4 MeV have been studied by the ${}^{64}\text{Ni}(p,t){}^{62}\text{Ni}$ reaction at 40 MeV bombarding energy with an overall resolution of 12 keV FWHM. Spins and parities are assigned to levels which were excited with characteristic angular distributions. These include 0^+ states at 2.05, 2.89, 4.23, 4.62, 5.45 MeV. A distorted-wave analysis based on shell-model wave functions was performed and compared to the experimental differential cross sections.

NUCLEAR REACTIONS ${}^{64}\text{Ni}(p,t)$, $E = 40$ MeV; measured $\sigma(E_t, \theta)$; enriched target. ${}^{62}\text{Ni}$ deduced levels, L, J, π .

[†]Work supported in part by the National Science Foundation.

* Supported by CNRS (France). Present address: Institut des Sciences Nucleaires, B.P. 257 Centre de Tri, 38044 Grenoble-Cedex.

I. Introduction

The excitations and the level structure of the Ni-isotopes are of considerable interest for nuclear structure calculations. The closure of the $1f_{7/2}$ shell at ${}^{56}\text{Ni}$ leads to a description of the low-lying states with the proton shells completely inert and the valence neutrons in the $2p_{3/2}$, $1f_{5/2}$, $2p_{1/2}$, and $1g_{9/2}$ shells. Several detailed shell-model calculations have been performed by Auerbach,¹ Cohen et al.,² and Glaudemans, et al.³ within the $2p_{3/2}$, $1f_{5/2}$, $2p_{1/2}$ neutron configuration space.

Considerable experimental information exists of the levels of ${}^{62}\text{Ni}$ up to an excitation energy of 6 MeV. Information prior to January 1974 is summarized in the compilation of Verheul.⁴ Among the recent works, a great deal of new information concerning spin and parity values of many ${}^{62}\text{Ni}$ states has been provided using the ${}^{60}\text{Ni}(t,p)$,⁵ ${}^{64}\text{Ni}(p,t)$,⁶ ${}^{62}\text{Ni}(p,p')$,⁷ ${}^{61}\text{Ni}(p,p')$,⁸ and ${}^{62}\text{Ni}(n,\gamma)$ ⁹ reactions and the β -decay of ${}^{62}\text{Co}$ (ref. 10) and ${}^{62}\text{Cu}$ (ref. 11).

The present ${}^{64}\text{Ni}(p,t){}^{62}\text{Ni}$ experiment forms part of a systematic and high resolution study of the (p,t) reaction on the Ni-isotopes with the aim of determining the excitation energies, spins and parities of levels of the Ni-isotopes. Angular distributions were obtained from 6° to 54° for approximately 55 resolved levels in ${}^{62}\text{Ni}$ up to an excitation energy of 6.4 MeV. The characteristic features of the L-transfer in the angular distributions are used to make several new spin-parity assignments.

For both the initial and final nuclei, new shell-model calculations have been performed considering an inert ${}^{56}\text{Ni}$ core

and valence nucleons in the $2p_{3/2}$, $1f_{5/2}$, $2p_{1/2}$, and $1g_{7/2}$ shells where the number of the particles in the $1g_{7/2}$ orbit is limited to be not more than 2. The modified surface delta interaction (MSDI) was used as the effective two-body interaction in the calculations. The interaction strengths A and B as well as the single particle energy of the $1g_{7/2}$ orbit were adjusted to fit experimental ground state binding energies and level spacings. Details of calculations will be presented elsewhere.¹² Based on these, in the following referred to as the MSDI⁴ wave functions and the shell-model wave functions of Glaudemans et al.,³ (in the following referred to as MSDD3 wave functions), microscopic-distorted wave Born approximation (DWBA) calculations have been carried out and compared to the experimental data.

II. Experimental Procedure

The present experiment was performed with a 40 MeV proton beam from the Michigan State University Cyclotron in two different configurations. In one case, the reaction products were detected in a position sensitive wire-counter plastic-scintillator combination in the focal plane of the Enge split-pole magnetic spectrograph. The target used in this arrangement was a 0.38 mg/cm^2 thick, self-supporting ^{64}Ni foil (isotopic enrichment $\geq 99\%$). The energy resolution obtained was about 50 KeV FWHM. This configuration of detector and target allowed acquisition of very accurate angular distributions for a number of strong transitions and the tracing out of the deep minima of the $L=0$ angular distributions.

In the other experimental configuration the tritons were detected in Kodak NTB-25 photographic emulsions. Here the target was a 0.25 mg/cm^2 thick, self-supporting ^{64}Ni foil (isotopic enrichment $\geq 98\%$). The resolution of the system was optimized by adjusting the dispersion of the beam across the target while monitoring the resolution with the "speculator" system.¹³ A total resolution of about 12 KeV FWHM was obtained. In Fig. 1 a triton spectrum from the photographic plate data is shown.

In order to normalize the relative cross sections at different angles the beam on the target was monitored by recording the total charge collected in a Faraday cup and by recording the protons elastically scattered at 60° with a NaI-scintillation counter. These two methods agreed within a few percent. The absolute cross section was determined in two ways: One method was to measure directly the thickness of the thicker enriched ^{64}Ni -foil by weighing it, measuring the spectrograph solid angle and the charge collected in the Faraday cup, and then calculating the differential cross sections directly. The second method was similar except the $^{64}\text{Ni}(p,t)$ ground state transition was measured with thick natural Ni-foils which were weighed. These two techniques agreed within 5%. The accuracy of the absolute cross sections is expected to be within 10%.

III. Results

The excitation energies of the levels observed in the present experiment are given in Table 1. Also shown are results

from some of the previously published data on ^{62}Ni . Spin and parity assignments are indicated where they could be made from comparison to the angular distribution of low lying states with known spin, since the shapes of the angular distributions with the same L value change very little up to an excitation energy of 6.5 MeV. Values in parenthesis indicate less certain assignments.

Angular distributions were extracted for all transitions up to 6.45 MeV in excitation. They are shown in Figs. 2-4 according to the exhibited L-transfer.

A. L = 0 Transitions

Seven levels with excitation energies varying from 0.0 to 5.45 MeV were observed to be populated unambiguously by L = 0 transitions (see Fig. 2). Only four of these seven 0^+ states were previously known. For the 2.89 MeV level, Fanger *et al.*⁹ assign $J^\pi = 2^+$ from angular correlation measurements of $^{61}\text{Ni}(n,\gamma\gamma)$ radiations. A preliminary report by Davies, *et al.*⁶ regarding $^{64}\text{Ni}(p,t)$ angular distributions lists a 0^+ state near 2.85 MeV. In the present experiment an L = 0 angular distribution is unambiguously observed for the transition to a state at 2.889 MeV in agreement with Davies, *et al.* This may represent a conflicting result, since the 2.89 MeV level is the only one reported near this excitation energy in several studies which were carried out with an energy resolution of better than 10 keV. This puzzle can be solved by a high resolution $^{62}\text{Ni}(p,p')$ experiment ($E \leq 3\text{keV}$). For the transition

to the doublet at 3.518-3.523 MeV we observed a mixture of L = 0 and L = 2 angular distributions (see Fig. 2) indicating that one of these two states has spin and parity $J = 0^+$, the other $J = 2^+$. Here again the 0^+ assignment disagrees with the results of Fanger, *et al.*⁹ who resolved this doublet.

B. L = 2 Transitions

Fourteen levels are observed to be excited unambiguously by L = 2 angular distributions. Four other transitions show less clear L = 2 transfer patterns. The present 2^+ assignments agree in all cases with those of previous experiments and furthermore in some cases ambiguities have been removed from previous data.

The observed peak width in the triton spectrum for the 3.85 MeV transition indicates that this level is possibly a doublet. The summed angular distribution exhibit a predominantly L = 2 pattern. Fanger, *et al.*⁹ report two states at about this energy and assign 1^+ , 2^+ to the higher lying level of this doublet (see Table 1). Darcey, *et al.*⁵ observed in the $^{60}\text{Ni}(t,p)$ reaction an L = 0 angular distribution to this doublet affected by some admixture from other L transfers. The internal consistency of the (p,t) and (t,p) data suggests that there is a doublet at about 3.85 MeV in ^{62}Ni with spins and parities 0^+ and 2^+ in agreement with the $^{61}\text{Ni}(n,\gamma\gamma)$ ⁹ results. Different members of this doublet are then excited by the (p,t) and (t,p) reactions.

C. L = 4 Transitions

The angular distributions for ten transitions exhibit the characteristic features of L = 4 transfer (see Fig. 3.). Five other transitions have most probably L = 4 character. The present $^4_+$ assignments agree with those of previous investigations except for the level at 3.27 MeV for which Fanger, et al. quote $J = 1^+, 2^+$.

D. L = 3 Transitions

There are three cases of states excited by L = 3 angular distributions. Four other transitions show most likely L = 3 patterns. The key features for these identifications are the minimum near 30°, a second maximum at 35° and a sharp fall off from 40° to 50°.

IV. Distorted--Wave Analysis

Microscopic distorted-wave Born approximation (DWBA) calculations were made for the $^6\text{He Ni}(p,t)^{62}\text{Ni}$ reaction with the code DWUCK. The proton parameters were taken from the work of Liers, et al.¹⁵ Since no triton parameters were available for energies around 30 MeV, the ^3He parameters of Cage, et al.¹⁶ were used in the present analysis. The differences between triton and ^3He parameters have been found to be small.¹⁷ The optical parameters used in the present analysis are shown in Table 2. The DWBA calculations were normalized according to the procedure of Baer, et al.¹⁸ where

$$\left(\frac{d\sigma}{d\Omega}\right)_{\text{exp}} = 9.72 D_0^2 e (T_B \text{IN}_{B1} | T_a N_A)^2 (2J+1)^{-1} \sigma_{\text{DW}}^{LSJ}(0)$$

The quantity J is the total angular momentum of the transferred neutron pair. The Clebsch-Gordan coefficient accounts for the coupling of the isospin of the residual nucleus, T_B , to that of the transferred neutron pair to yield the isospin of the target nucleus, T_A . The factor D_0^2 is a normalization constant which arises from making the zero range approximation. The quantity e deals with the goodness of the wave function description of initial and final states and will be used to compare experimental transition strengths to those calculated from the nuclear wave functions used in the analysis.

Since only one value of the transferred orbital angular momentum L can contribute to a transition, the quantitative structure information available from the data is contained in the transition strength. The shapes of the angular distributions are essentially independent of details of the nuclear wave functions and are functions only of the L transfer and of the general features of the DWBA analysis used. The only, and simultaneously, strongest test of the wave functions is, therefore, their ability to predict the magnitude of the cross section. Ambiguities in the analysis of absolute cross sections arise, however, both from experimental errors and from uncertainties in the over-all normalization of zero-range DWBA calculations. Therefore, only comparative studies of several transitions with identical experimental and analytical techniques are meaningful. The success of the wave functions in describing

the initial and final states lies in the consistency with which the above introduced quantity ϵ remains close to unity for many states.

From the two sets of wave functions described above spectroscopic amplitudes have been calculated. The results are presented in Table 3 for various final states in ^{62}Ni .

The angular distributions obtained from the microscopic distorted-wave Born approximation (DWBA) calculations are compared in Fig. 5 to the experimental data. As shown, each calculated angular distribution is independently normalized for a best fit to the experimental data. In Table 4, the ratios of the experimental to the theoretical cross sections are presented. The normalization factor D_0^2 is chosen to yield $\epsilon=1$ for the ground state transitions and is equal to 31.6 (in units of $10^4 \text{ MeV}^2 \text{ fm}^3$) in the MSDI3 calculations and to 25.4 in the MSDI4 calculations. This last value is more close to the one reported by Casten *et al.*¹⁹ ($D_0^2=25$) and by Broglia *et al.*²⁰ ($D_0^2=23.5$) for nuclei ranging from Ca to Pb.

The relative strengths of transitions leading to the first 0^+ , 2^+ and 4^+ states are also better described by the MSDI4 wave functions. The second 0^+ state is not well accounted for by either of MSDI3 or MSDI4 wavefunctions. Since the MSDI3 wave function for this state contains more than 90% of seniority $v=4$ and $v=6$ components, the spectroscopic amplitudes (see Table 3) for the pick-up of two neutrons from the active orbits are very small resulting in a large underestimation of the transition strength. The MSDI4 wave function which is essentially of seniority $v=0$ (60%) overestimates the transition strength by a

factor of 5. It seems obvious from the present analysis of the transition to the second 0^+ state that reality lies between the prediction of the two sets of shell model calculations. The transition to the first 3^- state is underestimated by a factor of more than 2. Probably, the contribution of the $2d_{3/2}$ orbit not included in the model space is not negligible. The discrepancies between the experiment and both sets of shell model predictions become quite important for higher lying levels and could probably be explained by the core-particle contributions to the transitions.

V. Summary

The $^{64}\text{Ni}(p,t)^{62}\text{Ni}$ reaction was studied using both a proportional counter and nuclear emulsions to detect the tritons. Several new levels were observed up to an excitation of 6.5 Mev and many new spin parity assignments have been made. Microscopic distorted wave Born approximation (DWBA) calculations were performed using two different sets of shell-model wave functions. The first set was calculated³ from a model space which included 3 active orbits (e.g. $2p_{3/2}$, $1f_{5/2}$ and $2p_{1/2}$). In the second set,¹² the $g_{9/2}$ orbit was also taken into account. A MSDI interaction was used in both cases. The wave functions calculated in the larger model space gave a better fit to the experimental data for the lowest 0^+ , 2^+ and 4^+ states. But both calculations failed to reproduce the transition strength for higher lying levels.

Acknowledgments

The authors are indebted to Professors W. Benenson and B. H. Wildenthal for help and comments. One of us (D.H.K.) would like to thank Professors H. Blosser and F. Kashy for their hospitality at the Michigan State University Cyclotron Laboratory.

REFERENCES

1. N. Auerbach, Phys. Rev. 163, 1203 (1967).
2. S. Cohen et al., Phys. Rev. 160, 903 (1967).
3. P.W.M. Glaudemans, M.J.A. De Voigt and E.F.M. Stephens, Nucl. Phys. A198, 609 (1972).
4. H. Verneul, Nucl. Data 13, 443 (1974).
5. W. Darcey, R. Chapman and S. Hinds, Nucl. Phys. A170, 253 (1971).
6. W. G. Davies et al., RHEI/R/170 (1968).
7. P. Beuzit, J. Delaunay and J.-P. Fonan, Nucl. Phys. A128, 594 (1969).
8. R. G. Tee and A. Aspinall, Nucl. Phys. A98, 417 (1967).
9. U. Fanger et al., Nucl. Phys. A146, 549 (1970).
10. J. N. Mo, S. Ray and S. K. Mark, Nucl. Phys. A125, 440 (1969).
11. D. M. Van Patter, D. Neuffer, H. L. Scott, C. Moazed and P. F. Hinrichsen, Nucl. Phys. A146, 427 (1970).
12. D. H. Kong-A-Siou and B. H. Wildenthal to be published.
13. H. G. Blosser et al., Nucl. Inst. and Meth. 91, 61 (1971).
14. P. D. Kunz, Univ. of Colorado, unpublished.
15. H. S. Liers et al., Phys. Rev. C2, 1399 (1970).
16. M. E. Cage et al., Nucl. Phys. A183, 449 (1972).
17. P. P. Urone, L. W. Putt, H. H. Chang and B. W. Ridley, Nucl. Phys. A163, 225 (1971).
18. H. W. Baer et al., Ann. of Phys. 76, 437 (1973).
19. R. F. Casten et al., Phys. Rev. C4, 130 (1971).
20. R. A. Broglia, C. Riedel and T. Udagawa, Nucl. Phys. A184, 23 (1972).

TABLE CAPTIONS

Table I.--Energy levels of ^{62}Ni observed in $^{64}\text{Ni}(p,t)^{62}\text{Ni}$

reaction, compared with previous data
* possible doublet

- a) present experiment b) Ref. 5 c) Ref. 8 d) Ref. 9
e) Ref. 4 f) Ref. 10
g) $\sigma_{\text{rel}} = (\int d\sigma)_{\text{exp}} / (\int d\sigma)_{\text{gs}}$

Table II.--Optical potential parameters used in the DWBA calculation.

Table III.--Spectroscopic amplitudes calculated with shell-model wave functions; D3 and D4 denote, respectively, MSDI3 wave functions and MSDI4 wave functions (see text).

Table IV.--Comparison of experimental transition strengths with microscopic DWBA predictions (see text).

TABLE I.-- ^{62}Ni .

E_x (keV)		J^π		i_n		σ_{rel}
(p,t) ^a	(t,p) ^b	(p,t) ^a	(t,p) ^b	(n, γ) ^d	(d,p) ^c	(p,t) ^a (t,p)
0.0	0.0	0 ⁺	0 ⁺	0 ⁺	1	100. 100.
1172 (2)	1178	2 ⁺	2 ⁺	2 ⁺	1	39.3 11.5
2047 (2)	2055	0 ⁺	0 ⁺	0 ⁺	1	2. 3.1
2300 (2)	2308	2 ⁺	2 ⁺	2 ⁺	1 + 3	5.7 1.3
2333 (3)	2341	4 ⁺	4 ⁺	4 ⁺	1 + 3	16. 2.0
2889 (3)	2887	0 ⁺	0 ⁺	2 ⁺	1	5. 0.3
3053 (5)	3041	2 ⁺	2 ⁺	2 ⁺		0.6
3153 (5)	3155	2 ⁺	2 ⁺	2 ⁺		8.9 2.7
3172 (5)	3168	4 ⁺	(4) ^f	1 + 3		2.9
3252 (5)	3263	2 ⁺	(2 + 4)	1 ⁺ , 2 ⁺ , 3 ⁺	3	2.7 9.9
3271 (5)	3277	4 ⁺	(4) ^f	1 ⁺ , 2 ⁺	1	31.4
				1 ⁺ , 2 ⁺	1	
3465 (5)	3464					
3518 (5)	3519	0 ⁺ , 2 ⁺	2 ⁺	2 ⁺	3	0.3
				2 ⁺ , 3 ⁺	1	4.6 1.6
3751 (5)	3758	3 ⁻	3 ⁻	3 ⁻	1 + 3	6.1 16.
3853 [*] (6)	3857	2 ⁺	(0 ⁺ , 7 ⁺)	1 ⁺ , 2 ⁺	1	14.7 8.6
				2 ⁺		
3969 (5)	3979	2 ⁺	2 ⁺	2 ⁺	1	3.5 1.3
3997 (5)	3992	4 ⁺	4 ⁺	4 ⁺		1.9
4011 (5)	4012				(3)	
					1	
4049 (5)	4059	4 ⁺	(4, 5, 6) ^f	1 ⁺ , 2 ⁺	1	5.6 1.2
4154 ^g (6)	4159	(4 ⁺)	(4 ⁺)	2 ⁺ , 3 ⁺	3	2.1 6.2
4175	4179				1	
4209.	4209.					
4226 (5)	4225	0 ⁺				2.5
4315 (5)	4312			1 ⁺ , 2 ⁺		

TABLE II.

	V_0	r_0	a_0	W	W_D	r'	a'	V_s	r_s	a_s	r_c
Proton	47.92	1.156	0.705	3.82	4.75	1.292	0.668	1.88	0.94	0.853	1.25
triton	173.34	1.11	0.769	23.06	-	1.547	0.793	-	-	-	1.25

TABLE III.

J	$E_x(\text{MeV})$	$(f_5)^2$	$(p_3)^2$	$(p_1)^2$	$(g_9)^2$	
0_1^+	0.0	D4	-1.0197	-7158	-5498	.4895
	0.0	D3	1.0294	.7192	.5797	
0_2^+	2.75	D4	.1065	-.4658	.1229	.0060
	2.09	D3	-.0144	-.0444	.0425	
0_3^+	2.84	D4	-.2186	.4270	.0543	-.0078
	2.94	D3	-.2095	.5774	-.1014	
0_4^+	3.23	D4	.1939	.0111	-.2802	.0104
	3.25	D3	.2723	-.0606	-.3574	

	$(f_5)^2$	$(f_5 p_3)$	$(f_5 p_1)$	$(p_3)^2$	$(p_3 p_1)$	$(g_9)^2$		
2_1^+	1.71	D4	.5784	-.4580	.5579	.5126	.5181	-.0464
	1.45	D3	.6348	-.4889	.6870	.5264	-.5871	
2_2^+	2.64	D4	.2162	.7540	-.1232	-.0190	.5187	-.0033
	2.28	D3	-.1409	-.3471	.0371	-.0325	.4024	
2_3^+	2.87	D4	-.8655	-.2404	.1611	.3353	.5738	-.0079
	2.97	D3	-.3555	-.5949	-.1670	.4119	-.5226	
2_4^+	2.96	D4	-.2348	.8088	.6040	-.2895	-.2106	.0126
	3.04	D3	.8524	-.3428	-.6159	.0628	.1731	

	$(f_5)^2$	$(f_5 p_3)$	$(g_9)^2$		
4_1^+	2.38	D4	.8225	-1.5624	-.035
	2.37	D3	-.9633	1.5572	
4_2^+	2.83	D4	1.1489	1.0753	.0087
	2.87	D3	.7455	1.2355	
4_3^+	3.53	D4	.488	.0125	.0027
	3.26	D3	1.091	.3182	

TABLE III.--Continued.

	$(F_5)^2$	(F_3P_3)	$(E_3)^2$
4_4^+	3.81 D4	.1846 .0830	-.0004
	3.38 D3	-.4936	-.3127
		(F_5E_3)	(P_3E_3)
3_1^-	4.47 D4	-.0356	-.4966
3_2^-	4.72 D4	-.3820	.0305
3_3^-	5.21 D4	-.0676	-.1050
3_4^-	5.41 D4	+0.0771	-.0071

TABLE IV.-- ${}^6\text{Li}({}^4\text{He}(p,t)){}^6\text{Li}$.

J^π	E_x (MeV)			σ_{rel}	ϵ	
	Exp	D4	D3		D4	D3
0_1^+	g.s.	61.35	61.24	100	25.4±1	31.6±1
0_2^+	2.047	2.79	2.09	2	.2	37.
0_3^+	2.889	2.84	2.94	5	.81	.5
0_4^+	4.225	3.23	3.25	2.5	4.3	1.1
2_1^+	1.172	1.71	1.45	39	.83	.5
2_2^+	2.300	2.64	2.28	57	4.5	22.
2_3^+	3.053	2.87	2.97	0.6	.06	.04
2_4^+	3.153	2.96	3.04	8.9	3.5	3.
4_1^+	2.333	2.38	2.37	16	.63	.5
4_2^+	3.172	2.83	2.87	2.9	.54	.6
4_3^+	3.271	3.53	3.26	31	607.	358.
4_4^+	3.997	3.81	3.38	1.9	1214.	4.3
3_1^-	3.751	4.47		6.7	2.3	
3_2^-	4.650	4.72		1.7	25.	
3_3^-	4.994	5.21		1.9	19.	

FIGURE CAPTIONS

Fig. 1.--Triton spectrum from the $^{64}\text{Ni}(p,t)^{62}\text{Ni}$ reaction.

Fig. 2.--Angular distributions of L=0 and L=2 transitions observed in $^{64}\text{Ni}(p,t)^{62}\text{Ni}$ reaction.

Fig. 3.--Angular distributions of L=3 and L=4 transitions observed in $^{64}\text{Ni}(p,t)^{62}\text{Ni}$ reaction.

Fig. 4.--Angular distributions of transitions with undefined transferred angular momentum.

Fig. 5.--Comparison of experimental angular distributions with zero-range DWBA predictions.

